CHALMERS

Goeury Cedric

Modelling Whiplash Injuries using compressible CFD

Department of Applied Mechanics
Division of Fluid Dynamics/Division of Vehicle Safety
Chalmers University of Technology
Göteborg Sweden, 2008

Msc Thesis [2008 : 63]

Msc Thesis report 2008:63

Modelling Whiplash Injuries using compressible CFD

Msc Thesis report

Goeury Cedric

Department of Applied Mechanics
Division of Fluid Dynamics/Division of Vehicle Safety
Supervisors
Dr.Davidson Lars/Dr.Svensson Mats
Chalmers University of Technology
Göteborg, Sweden, 2008

Modelling Whiplash Injuries using compressible CFD
Msc Thesis report
Goeury Cedric

Msc Thesis report 2008:63
ISSN: 1652-8557

Department of Applied Mechanics,
Division of Fluid Dynamics/Division of Vehicle Safety
Chalmers University of Technology
Se-412 96 Göteborg, Sweden
Phone +46-(0)31-7721400
Fax: +46-(0)31-180976

Printed at Chalmers Reproservice
Göteborg, Sweden 2008

Msc Thesis
by
Goeury Cedric
Department of Applied Mechanics
SUPERVISORS
Dr.Davidson Lars/Dr.Svensson Mats
Division of Fluid Dynamics/Division of Vehicle Safety
Chalmers University of Technology

Abstract

A number of accident studies and claims statistics coming from the insurance industry clearly show that low severity rear impact can lead to neck injuries causing long term disorders. The work, originated from a hypothesis of Aldman (1986), proposed a pressure gradient injury mechanism during a swift extension-flexion motion of the cervical spine.

During a whiplash motion, a rise of velocity can be expected and pressure gradient can thus be expected to occur. An experiment using pigs [Svensson, 1993], which exposed pigs to a whiplash motion showed a peak of transient pressure at the middle of the cervical spine. Moreover, another study using mathematical model confirmed the same pressure shape.

The aim of this study is to validate the pressure effect theory on human beings during a rear-end impact using Computational Fluid Dynamics (CFD). The internal vertebral venous plexus is modeled as a 3-D pipe, which is radically rigid but axially flexible. In order to simulate the expanding of the pipe, the flow of blood is considered as a compressible flow. The efforts done in this work were directed in order to find a significant compressible pattern.

With the help of Fluent, we found a best Bulk modulus(B) which allows to obtain results without oscillation. The chosen bulk modulus corresponds to the bulk modulus of the blood vessel wall allowing to simulate the radius flexibility of the pipe. Then, the whiplash simulations have been carried out and, a negative pressure dip appeared at the middle of the cervical spine during the S-shape configuration. The results are compared to animals experiments and mathematical model in order to confirm them.

Keywords: whiplash injury, compressible flow, pressure transient, CFD

Acknowledgement

This work was carried as a cooperation project between the Fluid Dynamics Division and the Vehicle Safety Division, Department of Applied Mechanics, Chalmers University of Technology under the supervision of Dr.Davidson Lars and Dr.SvenssonMats.

I would like here to express my gratitude to the persons and institutions that made my internship possible at the Chalmers university of technology in Sweden :

Firstly, I would like to thank Chalmers University of Technology for giving me the opportunity to work in the ressearch area of Applied Mechanics, and to thank my school Matmeca (Engineering School in Mathematic Modelling and Mechanic) which allowed me to make this internship.

Secondly, I would like to express my sincere gratitude to my supervisors, Professor Lars Davidson and Professor Mats Svensson, for the great opportunity that they have given me allowing to make my internship in their division, their great support and encouragement, for their guidance and stimulating discussion during this work.

I would like to express thanks also to Yungfeng Yang for giving me a good introduction to the problem when I was starting here and also helping me in the later stage of the project. I would also like to thank Fredrik Carlsson, Fluent Sweden AB, who provided forceful technical support.

And I would like to thank, of course, all the people at the Department for their help, support and kindness who contributed to a very pleasant work atmosphere.

Nomenclature

List of abbeviations

AIS	Abbreviated Injury Scale
B	Bulk modulus
$C1 - C7$	Cervical Vertebrae (C1 at the top, C7 at the bottom)
CFD	Computational Fluid Dynamics
CNS	Central Nerve System
CSD	Computational Structure Dynamics
CSF	Cerebro Spinal Fluid
DRG	Dorsal Root Ganglion
g	Acceleration of gravity
NIC	Neck Injury Criterion
$PMHS$	Post-Mortem Human Subjects
Re	Reynolds Number
ρ	Density
μ	Dynamic viscosity
ν	Kinematic viscosity
τ_w	Wall shear stress
$T1$	First Thoracic Vertebrae
UDF	User Defined File
WAD	Whiplash Associated Disorders

Contents

Introduction

Neck disorders resulting from the transportation have a long history. A phenomenon called "concussion of the spine" was reported as early as 1862. Today, Whiplash Associated Disorders (WAD), often called whiplash injuries or AIS1 (AIS: Abbreviated Injury Scale) neck term suffering for the occupant. The word whiplash describes possible neck motion in eight cases of neck injuries arising from motor vehicle crash.

Whiplash Associated Disorders represent one of the most significant type of injuries in car crashes regarding both frequency and long-term consequences. The injury mechanism is not fully understood. A new model for explaining these injuries was presented by Aldman (1986). He claimed that the pressure gradient, caused by fluid motion under the shortening of the spinal canal at extension movement, give rise to damage to the nervous tissue of the Central Nervous System(CNS).

The aim of this study is to develop a compressible pattern using CFD, which is in agreement with the experimental results and the incompressible CFD results. The first part of this study is about the whiplash generality with the explanation and the stakes of the phenomenon. The second part deals with the methodoly in order to create a convenient pattern for the CFD study. And the last one is about the results of simulations and the discussion of these ones compared to the experimental results.

Chapter 1

Whiplash phenomenon: explanation, stakes and hypothesis

1.1 Whiplash motion

Rear-end car collisions typically occur in traffic situation with dense traffic and relatively small distances between vehicles in the same lane. A sudden deceleration in the traffic tempo and the risk is significant that a driver will start to brake a little too late and with some residual speed bump into the vehicle in front.

During a rear-end car collision, the struck vehicle is subjected to a forceful forward acceleration and the car occupant is pushed forward by the seat-back. The head lags behind due to its inertia, forcing into a swift extension motion. Actually, this lag motion places the upper cervical segments in flexion, and lower cervical segments in extension: the cervical spine adopts the 'S-shape curve'. And when each part of cervical segments respectively obtain their maximal configuration, the head begins to rotate. And the upper cervical segments go from maximun flexion into extension whereas the lower cervical spine go from maximun extension into a less extension. This phenomenon is called 'Whiplash motion', it looks like a wave propagation on the cervical spine.

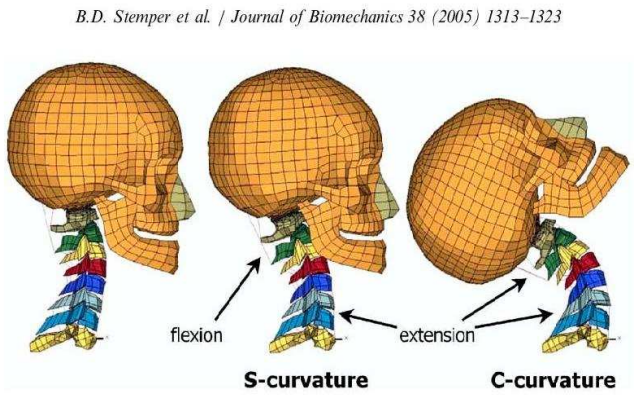

Figure 1.1: whiplash motion [B.D.Stemper et al., 2005]

1.2 Whiplash stakes

The symptoms of injury following neck trauma in rear-end collision include pain, weakness or abnormal responses in the parts of the body that are connected to the central nervous system by the cervical nerve roots.

In 1995, Quebec Tak Force (QTF) adopted a generic term 'Whiplash Associated Disosders'(WAD) to describe clinical symdromes and poorly symptoms associated with low speed rear-end collisions. WAD are classified into five classes based on clinical symptoms and signs:

QTF Grade	Clinical Presentation
0	No complaint about the neck, No physical sign
1	Neck complaint of pain, stiffness or tenderness only, no physical sign
2	Neck complaint and musculoskeletal signs Limited range of motion, point tenderness
3	Neck complaint and neurological signs Decreased deep tendon reflexes, sensory deficits
4	Neck complaint and fracture or dislocation

Table 1.1: Quebec classification of WAD [QTF,1995]

Neck injury is one of the most commonly reported injuries associated to the low speed rear-end impact. The cost of whiplash neck injuries is tremendous. In fact, in United States, the average cost per case of neck injury was $9,994$ of American dollars, arising an annual cost of $2,7$ billions of American dollars. In Europe, more than one million citizens suffer neck injuries involving social cost which are about 10 billions euros annually.

1.3 Adopted hypothesis in this study

After so much studies on the whiplash motion, there are three classes concerning hypothesis on whiplash injuries which are a hyperextension related hypothesis, facet joint related hypothesis and pressure gradient hypothesis.

However, Swedish Research has put up the hypothesis that relates whiplash injuries to pressure effects in the spinal canal of the cervical spine [Aldman, 1986] [1]. In fact, Aldman proposed a pressure change hypothesis, which is based on an increasing pressure in the spinal canal during the whiplash motion causing a compression on the nerve roots. This theory was investigated in several experiments with pigs [Svensson, 1993] [15]. These experiments have revealed that the pressure of the inter-vertebral canal increases and can injury the ganglion root at the lower of the cervical where the pressure transient is the most important.

Moreover, these results are corroborated with some symptoms of the whiplash. The aim of this study is to validate the pressure effect theory on human beings using CFD and to correlate CFD results with experiment results.

1.4 Anatomy of the human neck

In order to make an accurate pattern of the whiplash motion, we need to identify the parts of the neck which will be modeled. The human neck is composed by spinal cord, venous plexus, cervical vertebrae, ligaments, intervebrae disc, muscle and skin. However, the aim of this study is to investigate the pressure transient during the whiplash motion with CFD. Therefore, only the spinal cord and the structure of cervical venous system, which are concerned by the pressure transient, will be studied in this part.

1.4.1 Structure of the spinal cord

The spinal cord is an extension from the brain stem through the foramen magnum of the skull into the spinal canal. As CNS, spinal cord provides a two-way conduction pathway to and from the brain. Spinal cord is protected by the vertebral body, the cerebrospinal fluid, and the meninges. The single layered dura mater of the spinal cord, called the spinal dural sheath, is not attached to the bony wall of the vertebral column. Between the bony vertebrae and the dura sheath is a rather large epidural space filled with soft padding of fat and a network of veins.

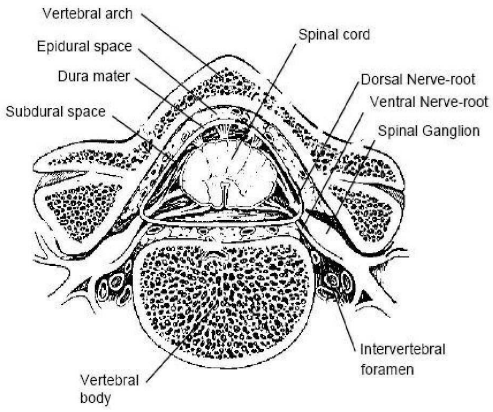

Figure 1.2: Cross section of the cervical spinal [Sance et al., 1984]

At each body segment spinal nerves arise. The spinal nerve carry motor fibres to the muscles and sensory fibres from the skin and musculoskeletal system. Each spinal nerve is associated with a section of the spinal cord in which the neurons are concerned with the sensory and motor activities of that nerve. The white matter of the spinal cord is formed of bundles of fibres carrying sensory information to higher centers or fibres of the motor system connecting the cerebral hemispheres, diencephalon and brainstem to the segmental neurons of the spinal cord. There is a high level of organization within the spinal cord. Both fibre bundles and nuclear groups are organized according to their participation in either sensory or motor, and according to which part of the body they are located. The dorsal half of the grey matter of the cord is concerned with the sensory activity while motor activity is concentrated in the ventral grey matter. Consequently, the dorsal roots of the spinal nerves are sensory, while the ventral roots are motor activity.

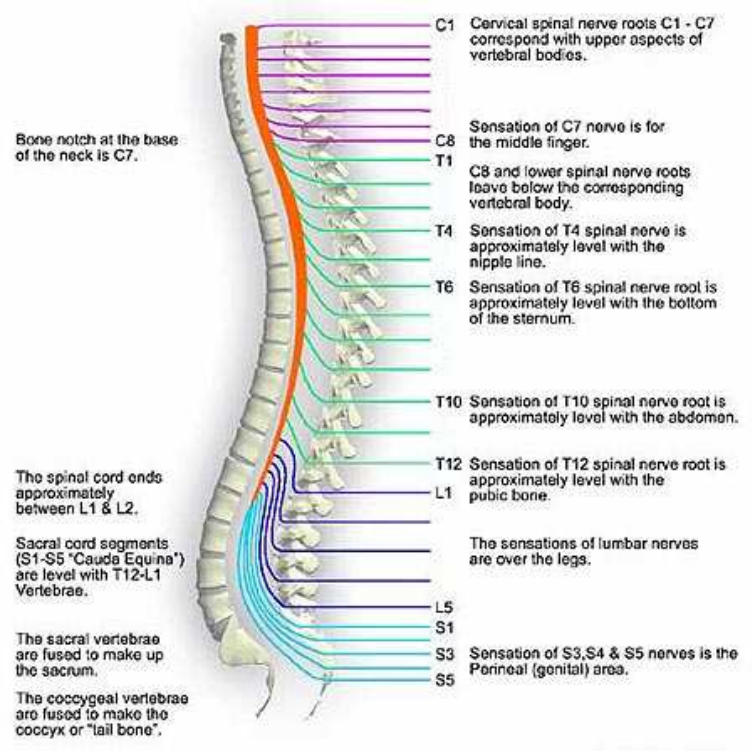

Figure 1.3: Cervical spinal nerves and pains distributions

As illustrated in figure 1.3, there are eight pairs of spinal nerves in neck. They are named according to their location from the spinal cord. The first seven pairs of cervical nerves exit the vertebral canal superior to the vertebrae for which they are named (C1-C7). C8 emerges inferior to the seventh cervical vertebrae. Moreover, nervous tissues are soft and delicate, consequently they can be injured by even slight pressure changes. Table A.1 at page c indicates any localized damage to the spinal cord or spinal roots associated with some form of function loss, either paralysis or parathesias.

1.4.2 Structure of cervical venous system

The veins which drain the blood from the vertebral column, the neighboring muscles, and the meninges form intricate plexuses extending along the entire length of the column. These plexus can be divided in two groups, external and internal, according to their positions inside or outside the vertebral canal.

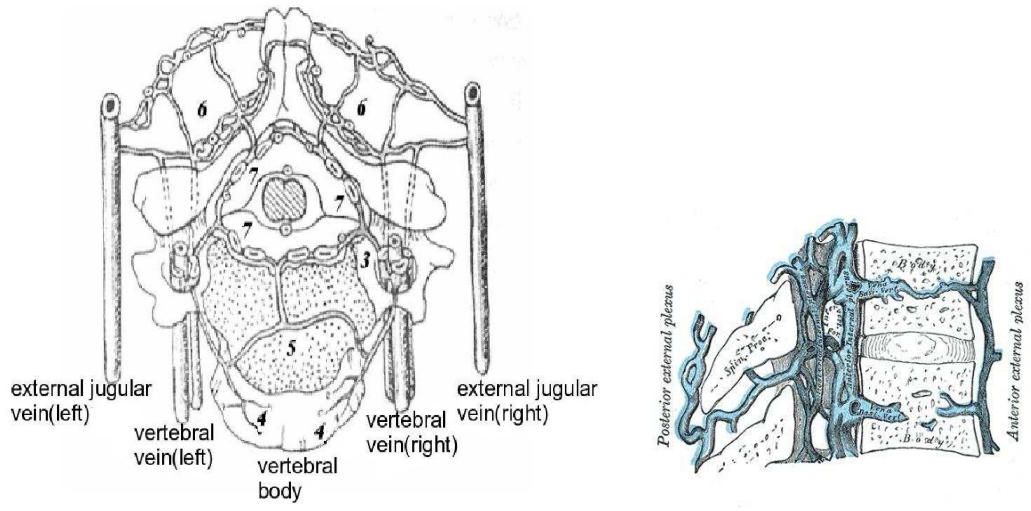

Figure 1.4: Cervical venous plexuses: intervertebral veins (3); basivertebrals (5); external cervival plexus (4 and 6); internal cervical venous plexus (7); [Clemens, 1961]

The internal vertebral venous plexus lie within the vertebral canal between the dura matter and the vertebrae, and receive tributaries from the bones and from the medulla spinalis. They form a closer network than the external plexus, and they run mainly in a vertical direction. The internal vertebral venous plexus communicates with the intracranial basilar venous plexus.

The external venous plexus lie in front of the bodies of vertebrae, and is formed by the main trunk of the external jugular vein and vertebral veins joining the plexus. It is located along anterior and posterior aspect of the vertebrae. They communicate with the internal vertebral venous plexus via segmental intervertebral veins and also receive tributaries from the deep and anterior cervical veins.

As mentioned above, external and internal venous plexus communicate through bridging veins which are called intervertebral veins. The intervertebral veins accompany the spinal nerves through the intervertebral foramina.

Due to extensive communication, vertebral venous plexus could serve as regulator to balance the volume and pressure changes of the cervical spine. Cervical venous system is obviously capable of passing large quantities of blood without developping varies. Since external and internal plexus of veins are associated with the vertebral column, the volume of change of the plexus can induce the pressure transient in the spinal canal. This pressure transient could generate a great strain stress that damage the root ganglion around the transverse foramen.

Chapter 2

Methodology

2.1 Theorical model

The lenght of the cervical canal changes during the whiplash motion. In fact, it decreases at extension and increases at flexion motion [Breig, 1978] [5].

That means that the inner volume of the spinal canal decreases during the neck motion and increases during flexion of the neck. Futhermore, in this study, the fluid flow is considered as compressible. Consequently, two phenomena will appear:

1. The fluid will be compressed and it will induce a variation of pressure. In fact, with the definition of the bulk modulus B, the variation of density can be relied on the variation of pressure:
$$B = -v\frac{\partial p}{\partial v} \tag{2.1}$$
and with the relation $v = 1/\rho$, this new equation is found:
$$B = \rho\frac{\partial p}{\partial \rho} \Leftrightarrow \frac{\partial p}{B} = (\frac{\partial \rho}{\rho}) \tag{2.2}$$

2. Moreover, the blood volume can move inside the spinal canal as well as between the inside and outside spinal canal and thus compensate for the change in inner volume of the spinal canal during the whiplash motion. Therefore, the venous blood, which forced flow in the vertebral venous plexus and its bridges will be undergone to rapid velocity changes which will generate a pressure transient.

The pressure transient is expected to increase the strain stress to the soft tissue in the intervertebral canals and cause injuries.

2.2 Modelling

2.2.1 Geometric model

Although Cerebro Spinal Fluid (CSF) can flow in and out the cervical spinal canal, due to the greater flow resistance in the subrachnoid space, the volume compensation of the CSF has been considered as minor importance [Svensson M.Y, et al., 1993] [15]. So, the main hypothesis is that the blood inside the cervical vertebrae is responsible for the pressure transient inside the spinal canal. To simplify the complex problem, the vertical vein of the venous plexus was lumped into a single pipe. This pipe is axially flexible. The internal vein descents along the spinal canal, it can be considered like a long straight pipe. The intervertebral veins, which go through the intervertebral foramen in transversal direction, connecte the internal venous plexus

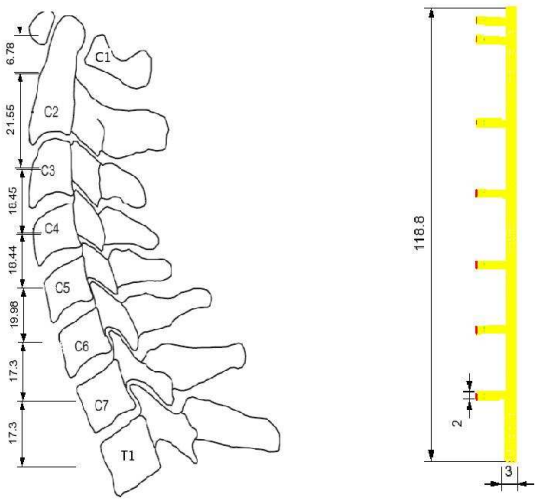

Figure 2.1: Geometric model: one vertical vein which descents along the central line of the spinal canal, with seven intervertebral veins

with the external venous plexus. The angles between the intrevertebral veins and the internal venous plexus are regarded as 90 degrees.

The vertical distance between each intervertebral veins corresponds to the distance of each vertebral body center. The lenghts of the internal venous plexus in the vertebrae is about 118.8 mm, including half the height of the first Thoracic vertebrae ($T1$). And the radius of the vertical vertebral vein and intervertebral veins are 1.5 mm and 1 mm respectively [Clemens,1961].

2.2.2 Kinematic model

In order to simulate the whiplash motion of the neck during the rear-end impact, data which describe the movement are essential. Ono (2000) [12] carried out some tests on human volunteer in order to analyse the neck motion during the whiplash. A volunteer was sitting in a rigid seat without headrest and he was restrained by a seat-belt. This test represents an 8 Km/h rear impact.

The movement of the neck can be divided in four phases:

- phase 1 (0 to 50 ms): No significant motion of the head and neck
- phase 2 (50 to 100 ms): the head moves backward in parallel to the torso and the neck shows the S-shape configuration.
- phase 3 (100 to 150 ms): The head starts to rotate backwards and the neck shows an extension motion
- phase 4 (150 to 300 ms): The rotational extension angles of the head and neck become maximum at 250 ms and then start to come back to their initial position.

Assuming the rotational angle is zero at the beginning, the overall movement of each vertebra can be evaluated by interpolation from the data in [12] using the software Matlab.

2.3 Compressible pattern

The blood is considered inside the vein like a compressible flow in order to simulate the flexibility of the pipe, in fact:

$$B = -v\frac{\partial p}{\partial v} \Leftrightarrow \partial p = -B(\frac{\partial v}{v}) \tag{2.3}$$

Moreover, the expression for v and ∂v are:

$$\partial v = 2\pi r \partial r h \tag{2.4}$$

$$v = \pi r^2 h \tag{2.5}$$

Where r and h are respectively the radius and the height of the pipe. So,

$$\frac{\partial v}{v} = 2\frac{\partial r}{r} \Leftrightarrow \partial p = -2B(\frac{\partial r}{r}) \tag{2.6}$$

We can see that a variation of the pressure leads to a variation of the radius of the pipe. Moreover, with the definition of the bulk modulus, and with this relation $v = 1/\rho$, a new equation is found:

$$B = \rho\frac{\partial p}{\partial \rho} \tag{2.7}$$

So, liquid density is not a constant but is instead a function of the pressure field. In order to stabilize the pressure solution for compressible flow in Fluent, an extra term related to the speed of sound function is needed in the pressure correction equation. Consequently, when you want to define a custom density function for compressible flow, the model must also include a speed of sound function. The definition of the speed of sound is:

$$c = \sqrt{\frac{\partial p}{\partial \rho}} \tag{2.8}$$

And, with (2.7), we find the speed of sound for a liquid:

$$c = \sqrt{\frac{B}{\rho}} \tag{2.9}$$

If we consider that $\partial\rho = \rho - \rho_{ref}$, we obtain the equation for the density function:

$$\rho = \frac{\rho_{ref}}{(1 - \frac{\partial p}{B})} \tag{2.10}$$

And if we replace this expression in equation (2.9), we obtain the equation for the speed of sound function:

$$c = \sqrt{(1 - \frac{\partial p}{B})\frac{B}{\rho_{ref}}} \tag{2.11}$$

2.4 Simulation

Fluent is used for the CFD simulation. The movement and the compressible property of the 3D vein are included to the software by User Define File (UDF file).

The vein model was meshed into 53753 cells by Gambit. The blood inside the vein was considered like a newtonian flow, with density of $0.0035 Kg/m^3$. The cranial end of the modes extends to the foramen magnum. The net flow trough the cavity is zero [Svensson et al., 1989] [2]. Thus, the cranial end of the spinal canal, the foramen magnum can be considered as a rigid wall. The blood can freely through the vein in both directions, so the boundary conditions for all ports are outlet vent. Firstly, only the bulk modulus coefficient is modified in order to simulate the flexibility of the pipe. After, the bulk modulus which gave best agreement with the experiments with pigs was chosen. The boundary conditions were chosen to be as close as possible to the experiments. The time step size was 0.1 ms. The blood flow direction is defined as positive when the blood flow upward along vertical vein, and flow out from intervertebral veins.

Chapter 3

Results

The entire simulation covered the time interval of 0.3 s. This interval corresponds to the time of the overall whiplash motion.

3.1 The Bulk Modulus

The bulk modulus B is defined like the inverse of the compressibility coefficient. This one appears in the compressible equation in the UDF files which define the compressibilty of the liquid. For this series of simulations, in order to simulate the resistance of veins, each port has been set outlet with a loss coefficient, 0.1 for the bottom of the main blood vessel and 100 for the top, 10 for intervertebral veins.

3.1.1 Simulation

A first series of simulation have been performed with different bulk modulus in each one. The bulk modulus is fixed for the first simulation to $1,3 \times 10^{10}$ Pa. This value corresponds to the bulk modulus of the blood. Then, this parameter is decreased by a factor of 10 at each simulation. Moreover, at each simulation, the pressure is determined as a function of time:

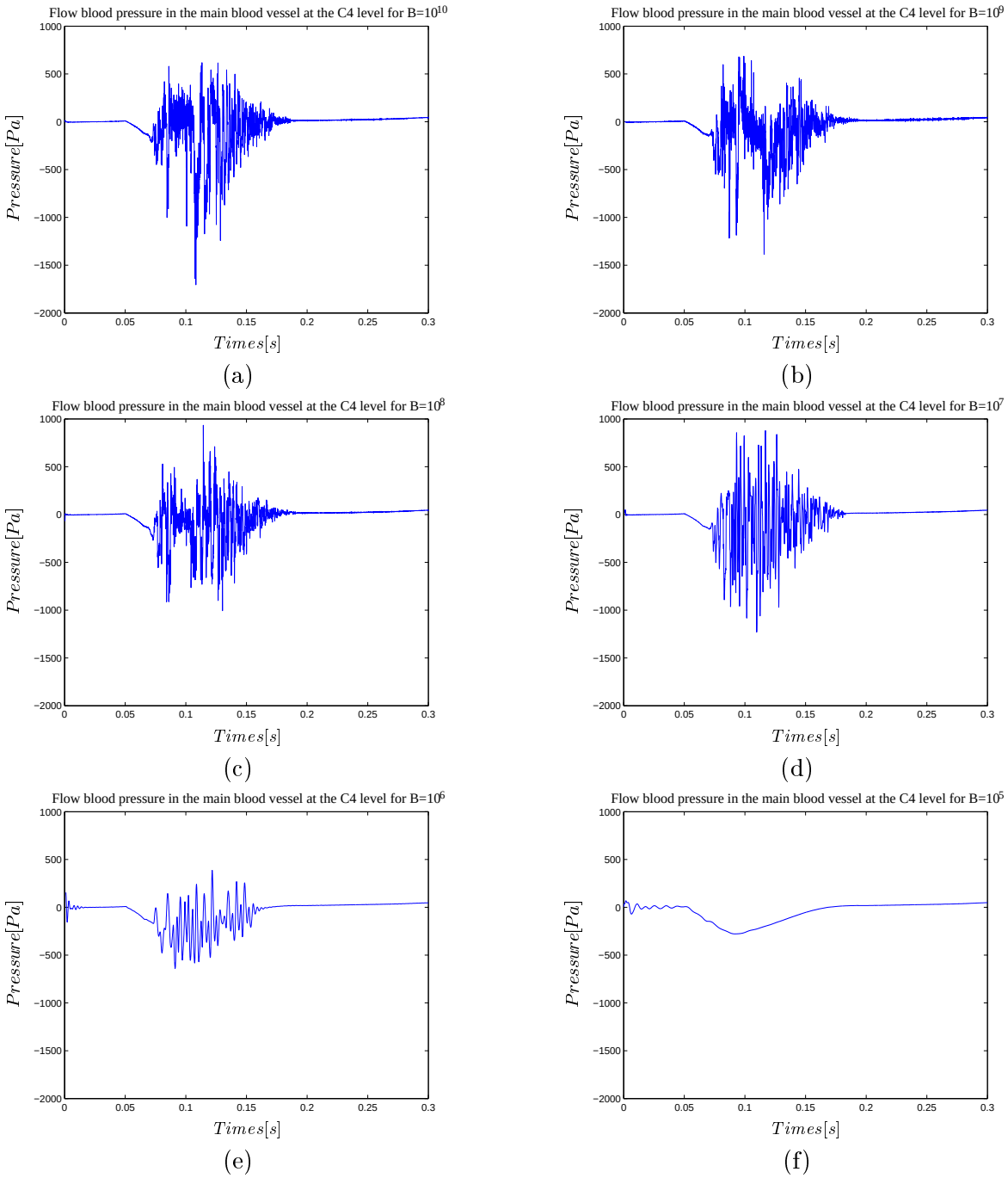

Figure 3.1: Bulk modulus evaluation: (a) Simulation for $B = 10^{10}$; (b) Simulation for $B = 10^9$; (c) Simulation for $B = 10^8$; (d) Simulation for $B = 10^7$;(e) Simulation for $B = 10^6$; (f) Simulation for $B = 10^5$

3.1.2 Observation and Explanation

The first phenomenon which can be noticed, is the effect of the bulk modulus on the pressure. Actually, the pressure amplitude decreases with a lower bulk modulus. This phenomenon can be explained by the Hook law applied to the blood vessel wall:

$$\sigma = E\epsilon \quad \text{with} \quad \begin{cases} \sigma = \text{tensil stress} \\ E = \text{modulus of elasticity} \\ \epsilon = \text{strain} \end{cases} \tag{3.1}$$

Moreover, there is a relationship between the bulk modulus B and the Young Modulus E:

$$B = \frac{E}{3(1-2\eta)} \quad \text{with} \quad \eta = \text{poisson coefficient} \tag{3.2}$$

Furthermore, $\eta \in [-1; 0.5]$, so $3(1-2\eta) = C$ is a constant, and the equation as follows is obtained:

$$\sigma = B\epsilon C \tag{3.3}$$

Consequently, a variation of the bulk modulus implies a variation of tensile stress σ which corresponds to the pressure in our case. So, if the bulk modulus decreases then, the pressure will decrease too.

Moreover, for each simulation, there are some oscillations which desappear with a bulk modulus $B = 10^5$ Pa. But, for this value and for bulk modulus $B = 10^6$ Pa, there is the presence of oscillations as soon as the beginning of the simulation. In order to find the reason of these oscillations, a spectral analysis is carried out using FFT in Matlab, the result is shown in figure 3.2 for bulk modulus $B = 10^6$ Pa:

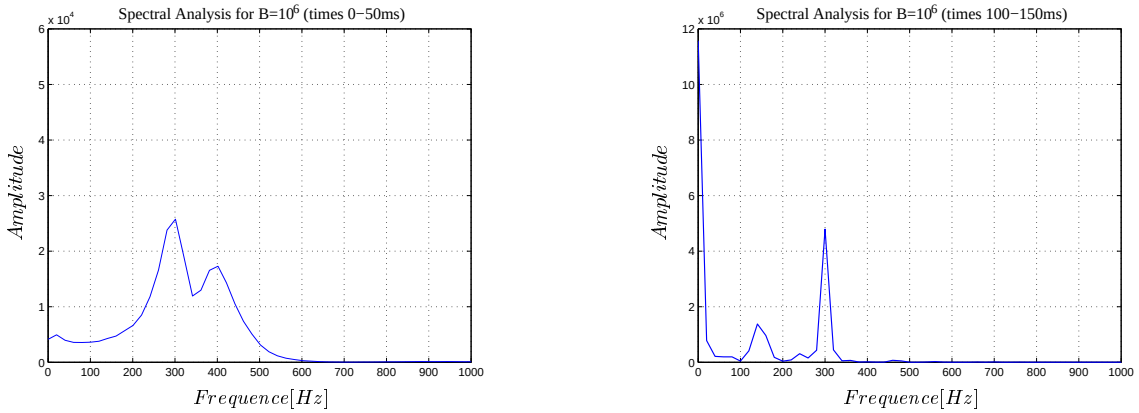

(a) (b)

Figure 3.2: (a) Spectral analysis at time 0 to 50 ms; (b) Spectral analysis at time 100 to 150 ms

Wave propagation is governed by the following relation:

$$v = f\lambda \quad \text{with} \quad \begin{cases} v = \sqrt{\frac{B}{\rho}} \\ f = \text{frequency} \\ \lambda = \text{wave length} \end{cases} \tag{3.4}$$

the wave length λ is deduced from this relation, and it corresponds to the length of the main pipe for the oscillations which occur during the time 0 to 50 ms and $t = 100$ ms to $t = 150$ ms. If we make the same study for the oscillations with the bulk modulus $B = 10^5$ Pa, the finding is the same. Moreover, the oscillations which appear at the beginning of the simulation for $B = 10^5$ Pa and $B = 10^6$ Pa can be explained due to the fluid pattern inside the pipe, which

is more close of a gas and there are less interactions between the atoms in a gas. So, it is easier to obtain a propagation of a perturbation when the pipe is submitted to a low tensile stress which can be induced by the jerky movement of the pipe. For the simulation with a higher bulk modulus at time 100 ms to 200ms, the same phenomenon can be generalized, because of the presence of oscillations at the same interval as the simulation with $B = 10^6$ Pa but due to so much oscillations, the spectral analysis of these simulations is more complicated and can be assumed to be caused by numerical problems.

3.1.3 Choice of the bulk modulus

In order to simulate the flexibility of the main blood vessel, the fluid inside the pipe will be assumed to have with the same elastic property as the elastic property of the arterial wall. The elastic modulus, E, of arterial wall is in the range 198 KPa to 912 KPa [Dongsheng Zhang, Dwayne D.Arola,(2004)] [7], with a poisson coefficient of 0.35. Therefore, the average elastic modulus is 5.52×10^5 Pa, and with the realation (3.2), the bulk modulus value is equal to 6.13×10^5 Pa. This value is chosen for the simulations which follow.

3.2 Whiplash simulation

In this part, the main resuts are presented, they correspond to the case where the top and the bottom have the same boundary condition in order to not give priority to the flow direction during the simulation, so, each port has been set as outlet with a loss coefficient, 0.1 for the bottom of the vein and for the top, 10 for intervertebral veins.

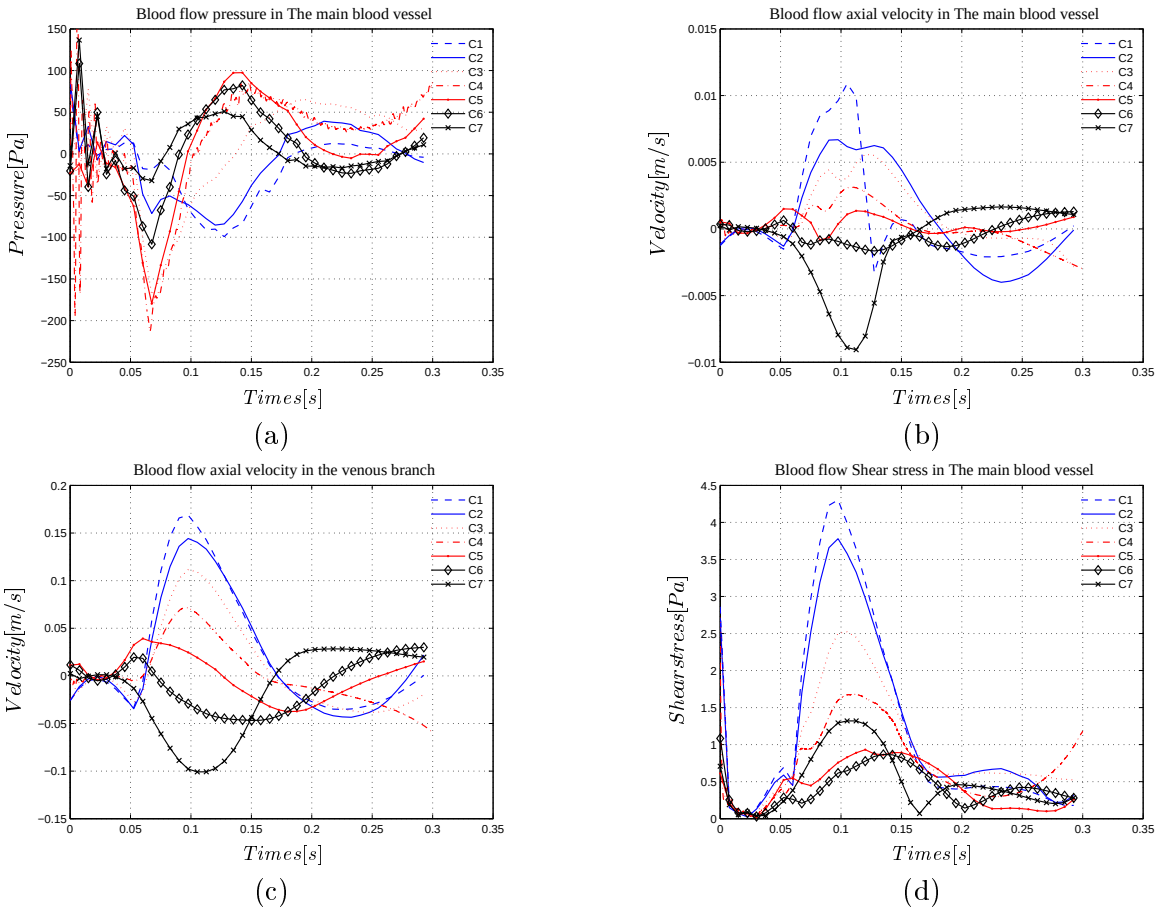

Figure 3.3: CFD calculation results: (a) pressure transient in the vertical vein; (b) blood velocity transient in the vertical vein; (c) blood velocity transient in the intervertebral veins, (d) shear stress transient of the intervertebral veins

The pressure was calculated for each cervical (C1-C7), in the main blood vessel. The result is shown in figure (3.3). The result shows some oscillations at time 0 to 50 ms which can be induced by the jerky movement of the pipe during the simulation (see part 3.1.2). Then, at 50ms, it is the beginning of the S-Shape configuration. A pressure drop appears at each level at time 70 ms, the pressures show the largest values at the lower half of the cervical spine and the lowest pressure is found at this time at the C4 level. This negative peak of pressure is about -210 Pa. Then, at time 100 to 150 ms, the pressure of the lower positions present a peak of pressure whereas for the upper positions, there is a valley of pressure. This phenomenon can be explained as follows.

In fact, at time 50 ms, the spinal canal begins to adopt the S-Shape configuration, that is to say, the lower cervicals are in extension whereas the upper cervicals are in flexion. The maximum of the S-Shape configuration appears at time 65 ms where the lowest rotational angle is found at the C3 level. Then, the spinal canal begins to extend and the lower cervicals go from a full extension to a less extension, so the volume of this part of the spinal canal increases and the pressure decreases. At the same time, the upper cervicals go from a full extension to an extension and induce a decrease of the volume which implies an increase of the pressure. The upper position pressures should present a positive peak due to these considerations, but there are only a negative peak for each position. According to Svensson (1993) [15], this might be explained by the fact that the effect of the volume expansion in the lower cervical spine dominates the compression of the upper cervical spine.

Furthermore, the flow of the fluid inside the main vessel has been studied. A change of direction is observed at time 60 ms and when it is the maximal S-shape configuration (70ms), the axial flow of the upper position is positive whereas for the lower position is negative. In fact, the positions C3, C4, C5 have the same axial velocity at this time and the difference of velocity between C1 and C4 is the same as the difference between the C4 and C7,

$$Vc1 - Vc4 = Vc4 - Vc7 \quad \text{with} \quad Vci = \text{velocity of the position Ci} \tag{3.5}$$

The same feature is observed for the C2 and C6 position. So, the velocity flows out and confirms the depressure to the main pipe at the middle of this one, that why the lower pressures are found at the C4, C3 and C5 positions.

Then, at time 100 to 150 ms, the spinal canal undergoes an extension which explains the peak of pressure for the lower cervicals. During the extension, the volume of the lower part of the spinal canal decreases and the pressure increases. But, the length of the spinal canal between C1 and C2 increases, and induces a decrease of pressure. This phenomenon can be explained by the experiment. When the head begins to rotate, it induces an elongation of the upper cervical. This movement of the neck induces a large decrease of the C1 velocity and a backflow which can be noticed at 125 ms to 140 ms, and a positive velocity for the side pipe. The fluid goes out through the side pipe and induces a depressure which can be noticed at time 130 ms (figure (3.3 (b))).

Chapter 4

Validation and Discussion

4.1 Validation

In this section, we will compare the present study with two other studies wich are relevant for this project, one study with pigs [Svensson, 1993] [15], and another one based on a mathematical model using finite element in order to calculate the pressure inside the spinal canal [Schmitt, 2000] [13].

4.1.1 Animals experiment

Anaesthetised pigs were exposed to a swift extension-flexion motion in order to simulate a whiplash motion [Svensson, 1993] [15]. For the pressure measurement transducers were used: one is used to measure the CSF pressure inside the skull, another measures the pressure at the C4 or C1 level and a last one which served as reference at the T1 level. The results show a valley of pressure at 70 ms at the C4 level as well as a positive peak pressure at 100 ms (figure 4.1). This study presents a similar shape of pressure for the C4 level, with a similar sharp negative peak of pressure which is followed by a positive peak of pressure.

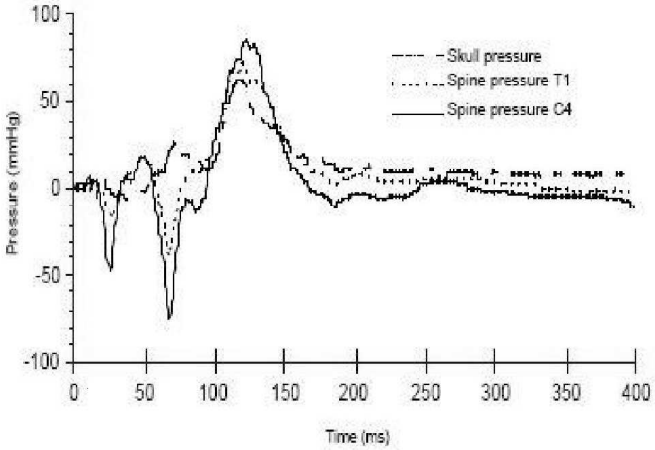

Figure 4.1: The pressure in the CNS versus time (Svensson, 1993)

However, the intensity of pressure in the present study is much lower than the Svensson's experiment. It can be explained the difference between the volunteer experiment and the pig experiment. In fact, with the pig experiment, the aim of the study was to see if a whiplash motion can injury a root ganglion of the spinal canal, so the intensity of the flexion and extension motion was very high. The aim of the volunteer experiment was to study the whiplash motion without causing any injury to the volunteer so, the pressure amplitude must be lower than the pig experiment.

4.1.2 Mathematical model

In his doctor thesis, Schmitt (2001) [13] developed a finite element (FE) model of the cervical spine in order to analyse the pressure phenomenon inside the cervical spinal canal. His model consists of the vertebrae, intervertebral discs, intervertebral joints, all major ligaments, neck muscles, and the head. It is built up of two parts, the solid model and the fluid model. The solid model consists of the seven vertebrae of the cervical spine and the first thoracic vertebra. A typical blood vessel of the internal venous plexus with diameter 2.5 mm embodies the fluid model. With aid of this FE model the pressure inside the blood vessel, the velocity flow field and the shear stress on the vessel wall could be calculated as functions of time. The pressure was analysed at the levels of C2, C4 and C6.

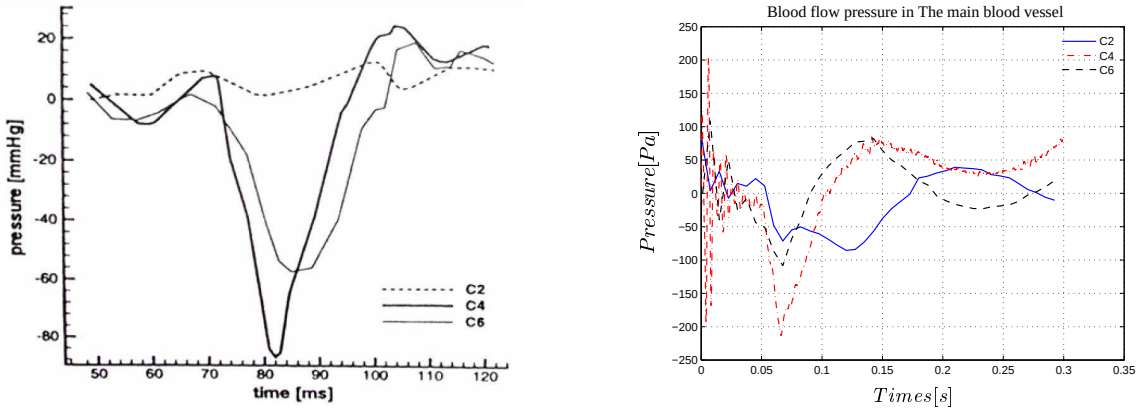

(a) (b)

Figure 4.2: (a) The mathematical model results; (b) The compressible CFD results

The present study shows a similare pressure variation for the cervicals C2, C4 and C6 as the mathematical study. In fact, in the present study, the position C4 and C6 present a negative peak of pressure which is followed by a positive peak of pressure whereas the position C2 has a small negative peak which is followed by another negative peak of pressure. Moreover, the lowest negative peak of pressure is found at the C4 level. The intensity of pressure in the current study is much lower than the mathematical model and the reason is that the motion of the head in the FE model is similar to the motion in the pig experiment.

4.2 Discussion

In this section, we will discuss of the influence of the boundary condition of the top face and the influence of the length of the intervertebral veins in order to improve the current pattern for future studies.

4.2.1 Boundary condition

Since there is limited litterature to provide reasonable loss coefficient for veins, the loss coefficient of the intervertebral veins in the current study was simply set to 10 and for the bottom 0.1. In this part, the loss top coefficient is investigated.

For the simulation with a high loss coefficient (100), the negative pressure peak is higher on the upper positions (figure (4.3 (a))). And the positive peak is very small compare to figure (3.3 (a)). Moreover, the pressure drop lags, in fact the lower pressure appears at time 90 ms whereas in the simulation with a loss coefficient at the top face equal to 0.1, the pressure drop is at time 70 ms.

Furthermore, when the top face condition is wall (figure (4.3 (b))), the negative pressure peak is found at the middle of the spinal canal and at time 70 ms. But, the pressure positive peak is very high and time for which the pressure is positive seems to be much longer in comparaison with the animals experiment.

The finding is as follows, when the loss top face coefficient is too high or when the top face condition is wall, the simulations cannot be considered. In fact, the shape of these curves are very differents to the animals experiment and the mathematical model.

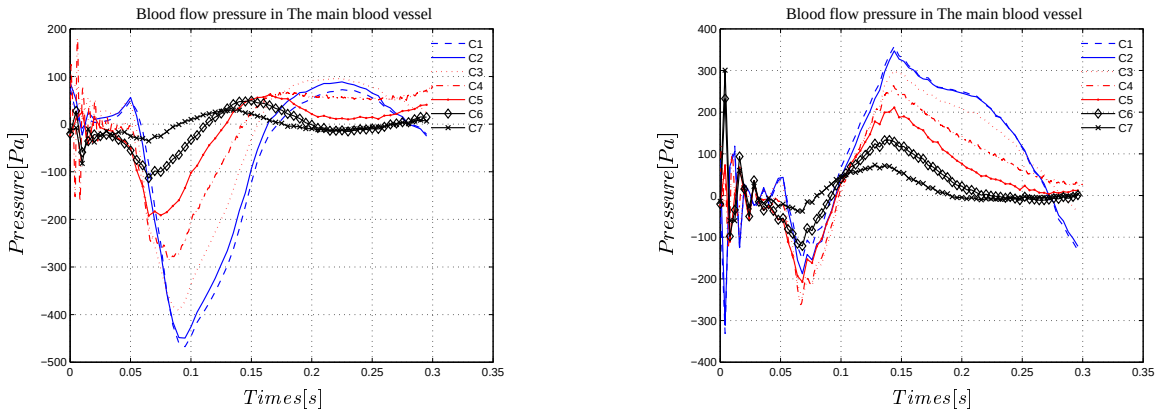

(a) (b)

Figure 4.3: CFD calculation results for different top conditions: (a) pressure transient in the vertical vein for a top loss coefficient equals to 100; (b) pressure transient in the vertical vein for a top wall condition

4.2.2 Lenght of the intervertebral veins

The length of the intervertebral veins influences the results (see figure D.1). Actually, the negative peak is close to the animals experiment and the shear stress intensity is higher when the side pipe is longer (See appendix D). Consequently, the influence of the length of the intervertebral veins is not be insignificant, in fact, the shear stress is expected to injury the root ganglion of the spinal cord. Generally, for arteries it is reported that the shear stress in flowing blood is of the order of 1 or 2 Pa [Schmitt, 2001]. In our case, the maximal value is about 4 Pa and can injury a root ganglion, but it is at the C1 position and not at the C4. But, in the human neck, the root ganglion is protected by another liquid: the dura matter, and the effect of the shear stress of the intervertebral veins on this liquid is unknown. So, the current study cannot assess whether the shear stress can damage a root ganglion during the whiplash motion.

Conclusion

In order to elucidate the injury mechanism, a compressible fluid flow inside a venous blood vessel was analysed. To verify Aldman's hypothesis, CFD simulation thanks to Fluent is used to find out the pressure transient in the spinal canal.

To obtain a reliable results, the efforts were directed to find a bulk modulus (B) which give results without pressure oscillation and to simulate the flexibility of the main blood vessel during the whiplash motion. This coefficient corresponds to the bulk modulus of the blood vessel wall.

The results indicate a pressure drop at the C4 level around 70 ms which corresponds to a time slightly after the maximal S-Shape configuration, as estimated by the volume change analysis. This pressure amplitude is the highest in the entire simulation.

The rotational angle of each cervical is less than 10 degrees whenever a negative pressure peak appears. The WAD injuries were decreased only by 20 percent [Nygren et al., 1985] when the car manufacturers introduce the head restraints. Therefore, in order to avoid whiplash injury, it necessary to limit the S-Shape deformation in order to limit the volume variation after the S-Shape configuration which seems to be responsible for the pressure drop.

Bibliography

[1] Aldman, B. *An analytical approach to the impact biomechanics of head and neck injury.* 30^{th} Proceedings of the Association for the Advancement of Automotive Medicine, pp.39-454. American Association for Automotive Medicine, Arlington Heights, IL 1986

[2] Aldman, B., Svensson, M.Y., Lövsund, P., Seeman, T., Örtengren, T. *A Theorical Model for a Pilot Study regarding Transient Pressure Changes in the Spinal Canal under Whiplash Motion.* Gothenburg, Sweden 1989

[3] Böstrom, O., Svensson, M.Y., Aldman, B., Hansson, H.A., Håland, Y., Lövsund, P., Seeman, T., Sunesson, A., Säljö, A.,Örtengren, T. *A new neck injury criterion canditate-base on injury finding the cervical spinal ganglion after experimental neck extension trauma.* IRCOBI 1996

[4] Brain, D.S., Narayan, Y., Frank, A.P *Gender dependent cervical spine segmental kinematics during whiplash.* Journal of Biomechanics, 36, 1281-1289 2003

[5] Breig, A. *Adverse Mechanical Tension in the Central Nervous System.* Almquist and Wiksell Int., Stockholm, Sweden, ISBN 91 – 2200126 – 3 1978

[6] Deng, B., Begeman, P.C, Yang, K.H., Tashman, S., King, A.I. *Kinematics of Human Cadaver Cervical Spine During Low Speed Rear-End Impacts.* 44^{th} Stapp Car Crash Conference 2000

[7] Dongsheng, Z., Dwayne, D.A. *Application of digital image correlation to biological tissues.* Almquist and Wiksell Int., Stockholm, Sweden, ISBN 91 – 2200126 – 3 1978

[8] Eichberger, A., Darok, M., Steffan, H. *Pressure measurements in the spinal canal of post-mortem human subjects during rear-end impact and correlation of results to the neck injury criterion* . Accid Analysis Prev.; 32:251-260. 2000

[9] Feng, L., Yang, J. *Modeling of Whiplash Injuries using CFD.* Master Thesis at Chalmers University of Technology, Gothenburg, Sweden 2008

[10] Nygren, Å., Gustafsson, H., Tingvall, C. *Effects od Different Types of Headrests in Rear-End Collisions.* SAE paper no.856023, 10th Int. Conference on Experimental Safety Vehicles, pp.85-90, NHTSA, USA 1985

[11] Ono, K., Ejima, S., Suzuki, Y., Kaneoka, K. *Prediction of the Neck Injuy Risk Based on the Analysis of Localized Cervical Vertebral Motion of Human Volunteers during Low-Speed Rear Impacts* . IRCOBI september 2006

[12] Ono, K., Kanoeka K., Wittek, A., Kajzer, K. *Cervical Injury Mechanism Based on the Analysis of Human Cervical Vertebrae Motion and Head-Neck-Torso Kinematics During Low Speed Rear Impacts.* Frontiers in Whiplash Trauma, vol 38, p372-p388 2000

[13] Schmitt, K.-U., Muser, M., Niederer, P., Walz, F. *Pressure Abberations Inside the Spinal Canal During Rear-end Impact*. Pro.International Congress on Whiplash Associated Disorders. 2001

[14] Sundararajan, S., Prasad, P., Demetropoulos, C.K., Tashman, S., Begeman, P.C., Yang, K.H., King, A.I. *Effect of Head-Neck Position on Cervical Facet Stretch of Post Mortem Human Subjects during Low Speed Rear End Impats*. Stapp Car Crash Journal, vol.48 2004

[15] Svensson, M.Y. *Neck-Injuries in Rear-End Car Collisions-Sites and biomechanical causes of the injuries, test methods and preventive measures*. Doctor Thesis at Crash safety division at Chalmers University of Technology, Gothenburg, Sweden 1993

Appendix A

Cervical spinal nerves and pains distributions

Disc Level	Nerve Root	Sensory distribution	Radicular Pain Distribution
C2/C3	C3	Posterior upper neck, occiput ear	Posterior upper neck, occiput
C3/C4	C4	Base of the neck, medial shoulder	Neck, upper scapula
C4/C5	C5	Lateral upper arm	Scapula border, lateral upper arm
C6/C7	C6	Bicep area, lateral forearm, thumb and 1^{st} finger	Lateral forearm, thumb and 1^{st} finger
C7/C8	C7	Posterior forearm, middle finger, middle finger	Scapula, posterior arm, dorsum of forearm, 3^{rd} finger
C8/T1	C8	Ulnar forearm and 5^{th} finger	Shoulder, ulnar forearm, 5^{th} finger

Table A.1: Cervical spine nerves and pains distributions [Schnuerer A.,et al.,2003]

Appendix B

Lenght and rotational angle of cervicals during the whiplash motion

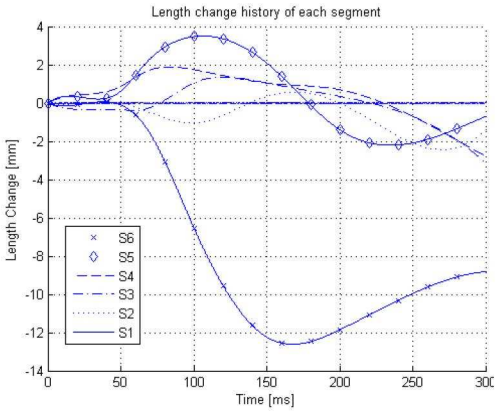

Figure B.1: Lenght of cervical segments during the whiplash motion

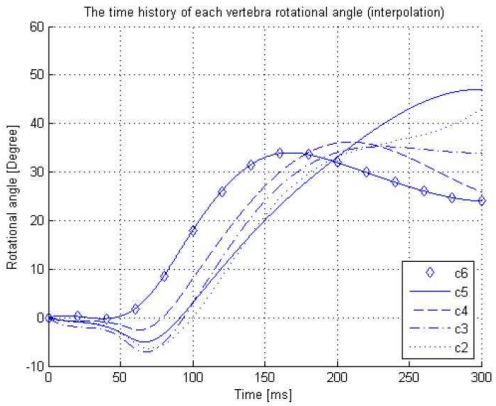

Figure B.2: Rotational angles of cervicals during the whiplash motion

Appendix C

Top face boundary conditions

In this part, the top face boundary condition is investigated. So, each port has been set outlet with a loss coefficient, 0.1 for the bottom of the vein and 10 for intervertebral veins, and the top boundary condition is changed.

C.1 Loss coefficient 100

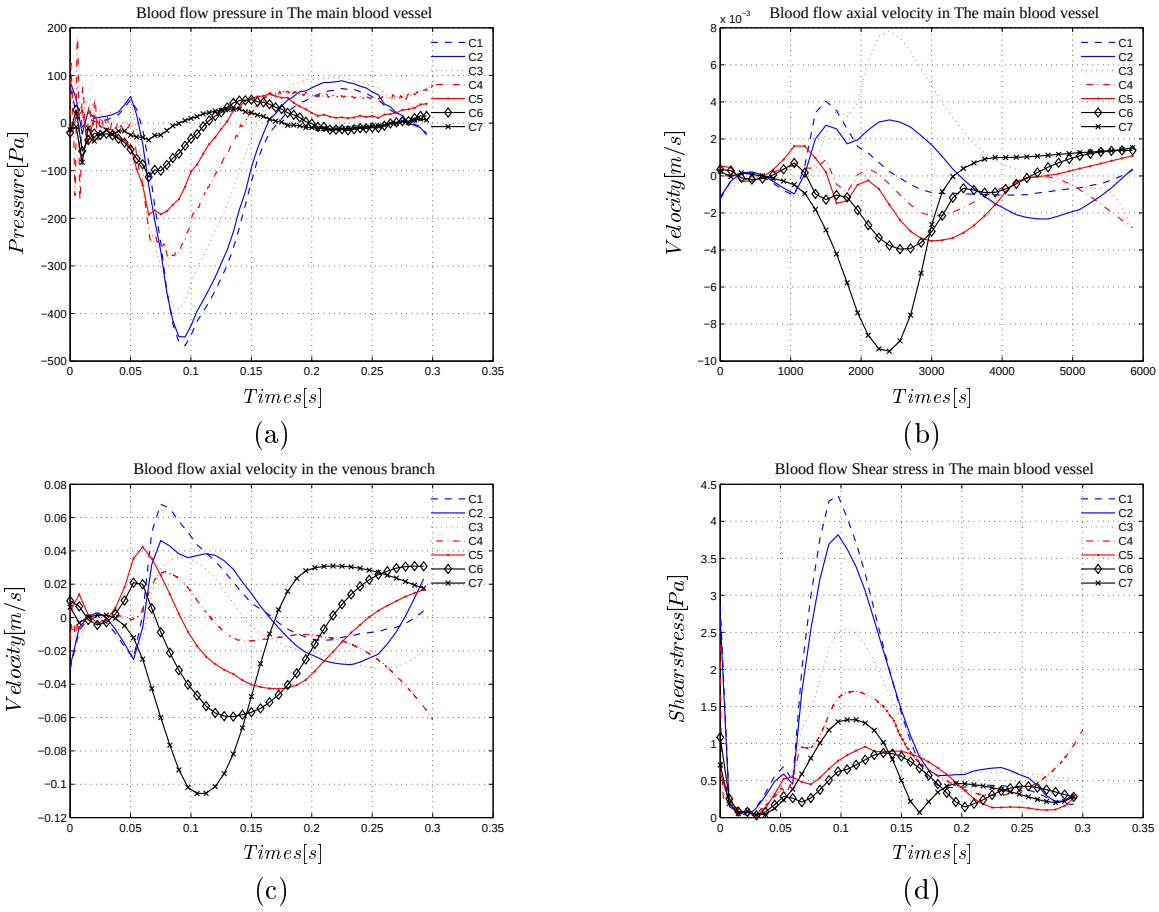

Figure C.1: CFD calculation results: (a) pressure transient in the vertical vein;(b) blood velocity transient in the vertical vein; (c) blood velocity transient in the intervertebral veins, (d) shear stress transient of the intervertebral veins

C.2 Top wall boundary condition

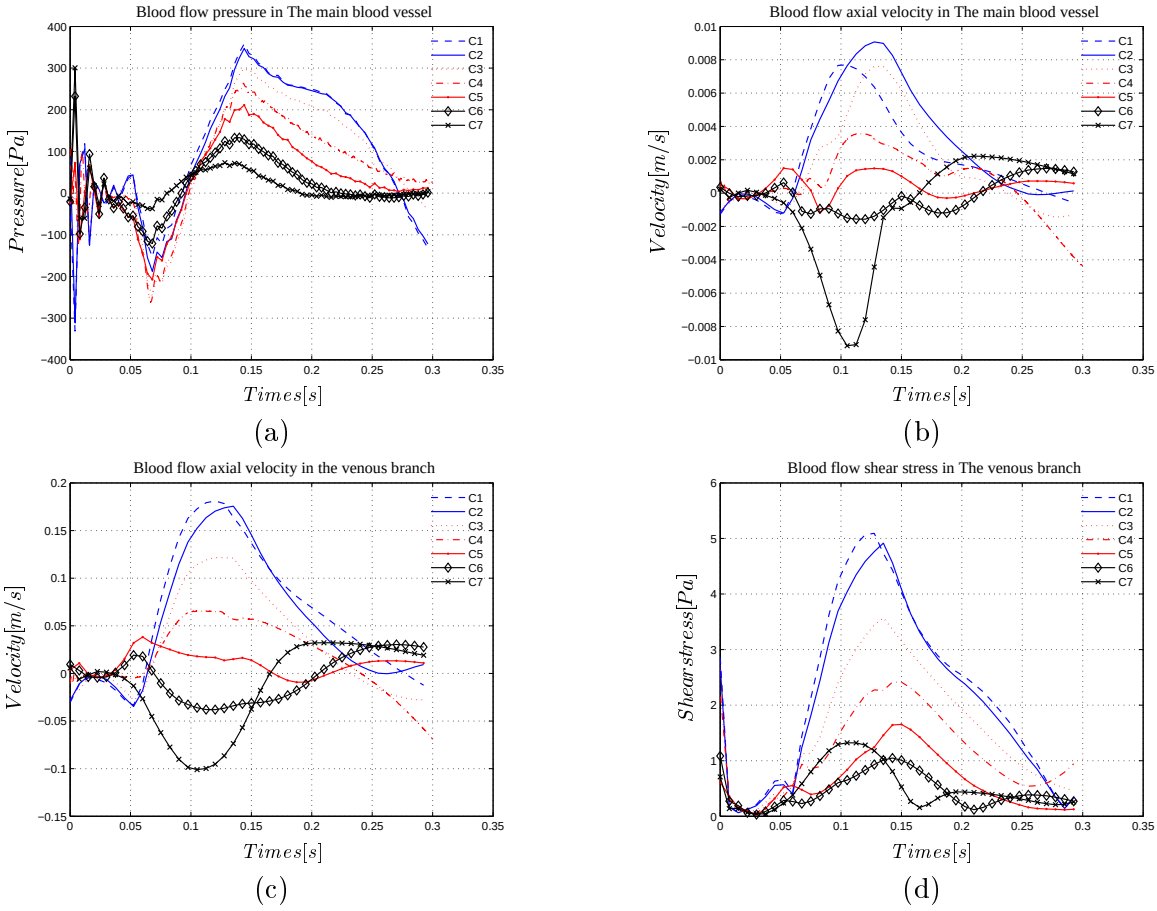

Figure C.2: CFD calculation results: (a) pressure transient in the vertical vein;(b) blood velocity transient in the vertical vein; (c) blood velocity transient in the intervertebral veins, (d) shear stress transient of the intervertebral veins

Appendix D

Lenght intervertebral veins

In this part, the lenght of intervertebral veins is investigated. So, each port has been set outlet with a loss coefficient, 0.1 for the bottom and the top of the vein and 10 for intervertebral veins. The intervertebral veins are reduced in order to see the lenght influence the result previously found.

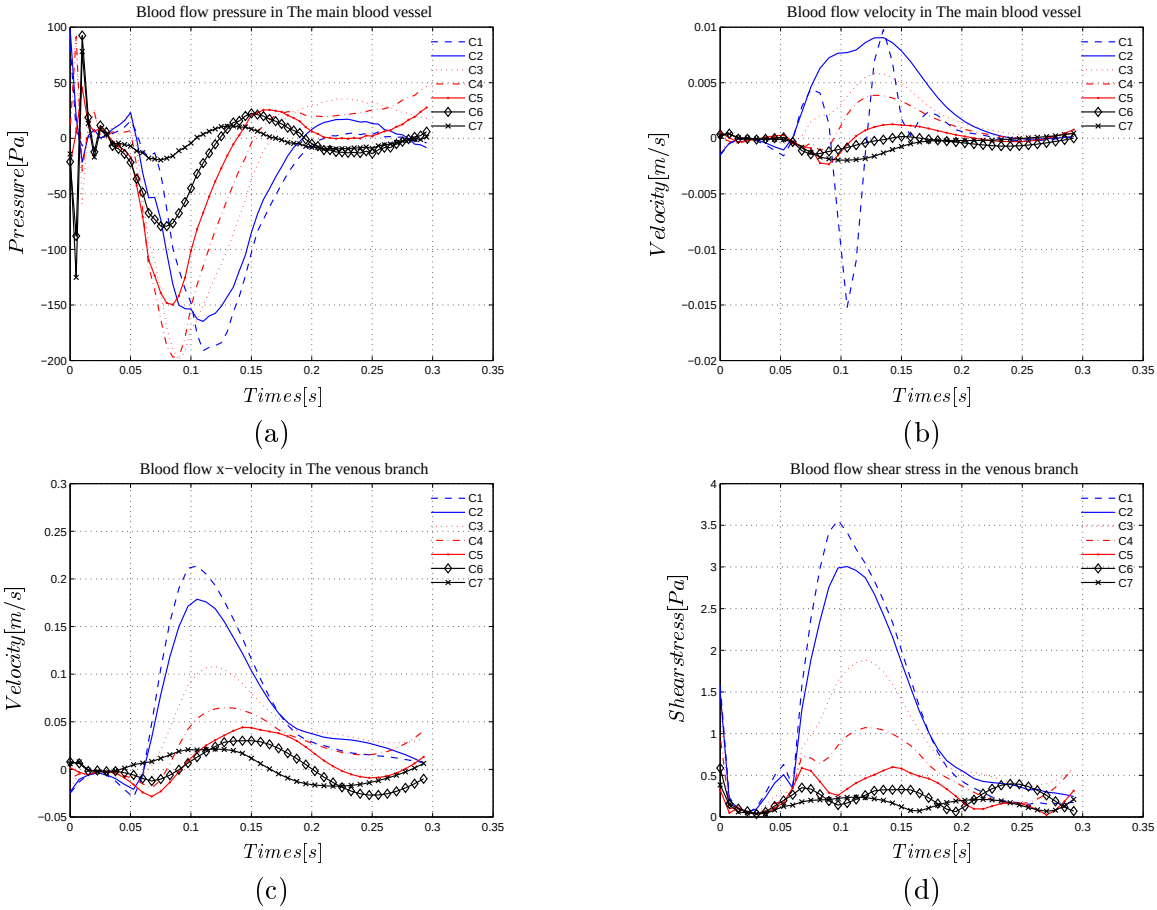

Figure D.1: CFD calculation results: (a) pressure transient in the vertical vein; (b) blood velocity transient in the vertical vein; (c) blood velocity transient in the intervertebral veins, (d) shear stress transient of the intervertebral veins

Appendix E

Simulation results

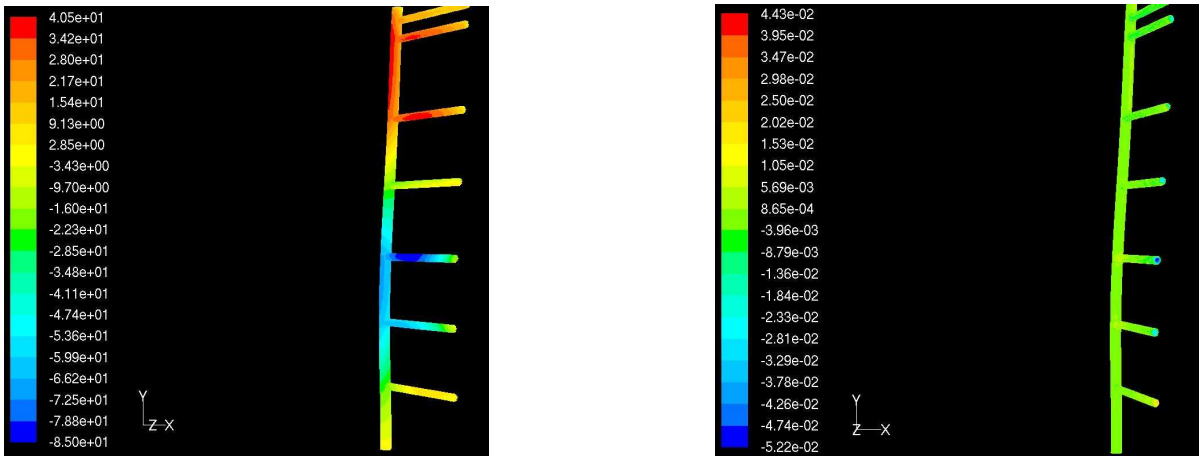

(a) (b)

Figure E.1: CFD simulation at time 50 ms: (a) Static pressure contour, (b) Axial velocity contour

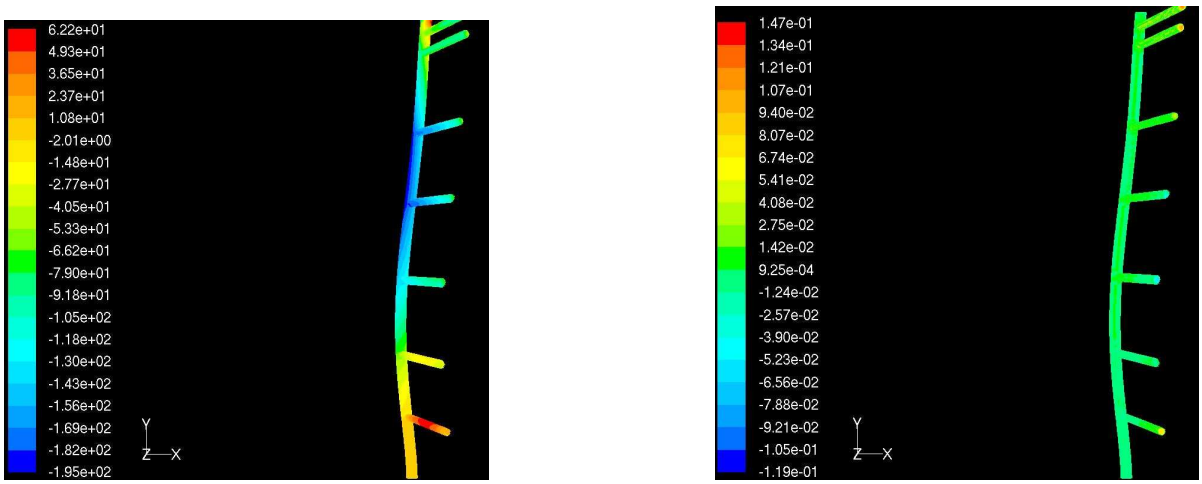

(a) (b)

Figure E.2: CFD simulation at time 75 ms: (a) Static pressure contour, (b) Axial velocity contour

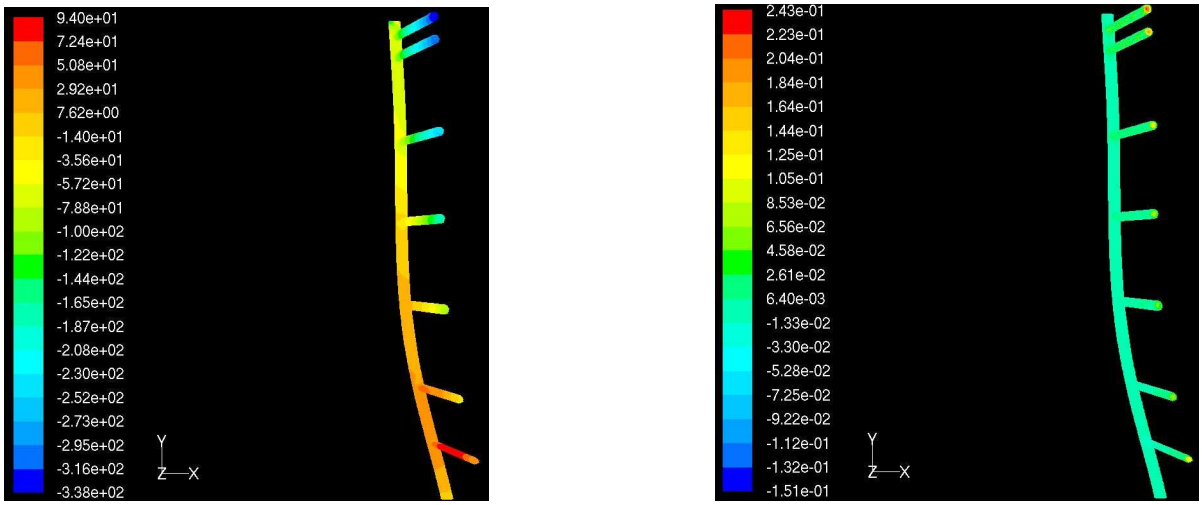

(a) (b)

Figure E.3: CFD simulation at time 100 ms: (a) Static pressure contour, (b) Axial velocity contour

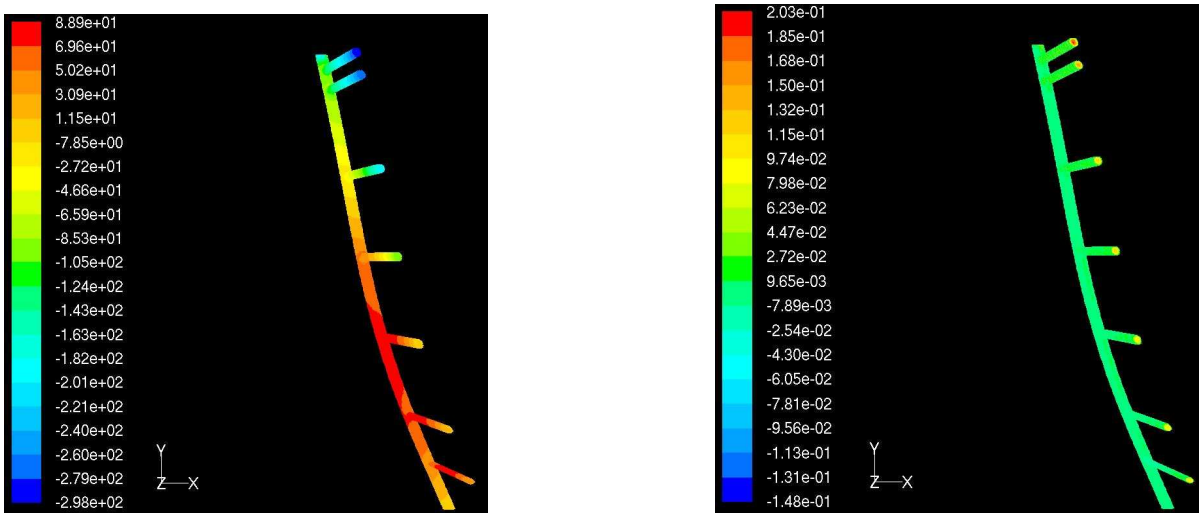

(a) (b)

Figure E.4: CFD simulation at time 125 ms: (a) Static pressure contour, (b) Axial velocity contour

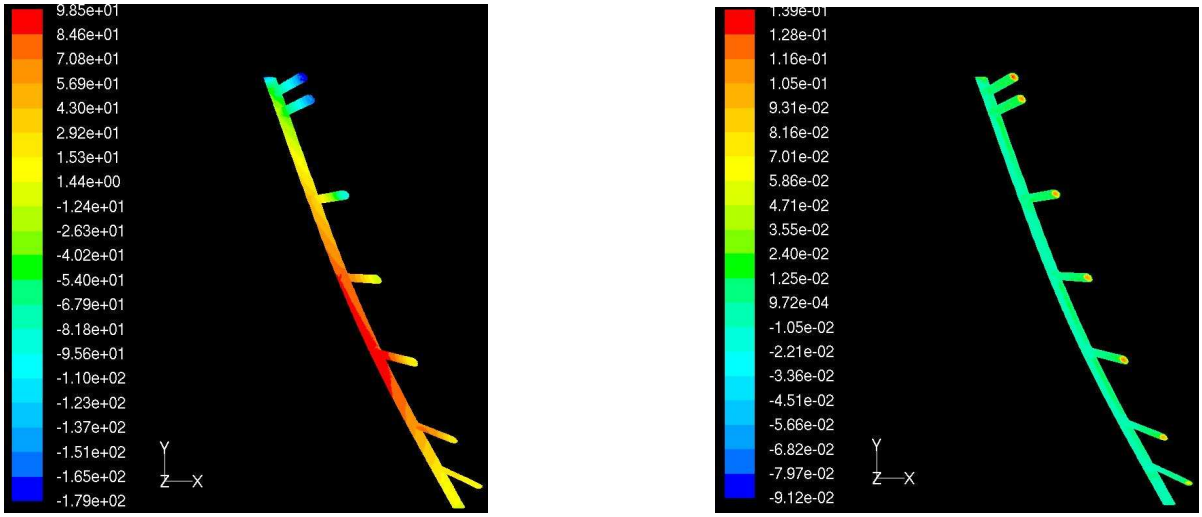

(a) (b)

Figure E.5: CFD simulation at time 150 ms: (a) Static pressure contour, (b) Axial velocity contour